Extended de Gennes Regime of DNA Confined in a Nanochannel

Liang Dai,[†] Johan van der Maarel,[†,‡] and Patrick S. Doyle*[†,§]

[†]BioSystems and Micromechanics (BioSyM) IRG, Singapore-MIT Alliance for Research and Technology (SMART) Centre, 1 CREATE Way, Republic of Singapore 138602

[‡]Department of Physics, National University of Singapore, 2 Science Drive 3, Republic of Singapore 117551

[§]Department of Chemical Engineering, Massachusetts Institute of Technology (MIT), Cambridge, Massachusetts 02139, United States

ABSTRACT: Scaling regimes for polymers confined to tubular channels are well established when the channel cross-sectional dimension is either very small (Odjik regime) or large (classic de Gennes regime) relative to the polymer Kuhn length. However, experiments of confined polymers using DNA as a model system are usually located in the intermediate region between these two regimes. In the literature, controversy exists regarding the existence of the extended de Gennes regime in this intermediate region. Here we use simulations and theory to reconcile conflicting theories and confirm the existence of extended de Gennes regime. We show that prior work did not support the notion of this regime because of the use of a wrong confinement free energy. In a broad sense, the extended de Gennes regime corresponds to the situation when excluded volume interaction is weaker than thermal energy. Such a situation also occurs in many other cases, such as semidilute polymer solutions and polymers under tension. This work should benefit the practical applications of nanochannels to stretch DNA, such as deepening the understanding of the relationship between the chain extension and channel size and providing the scaling behaviors of recoiling force for DNA at the entrance of nanochannels.
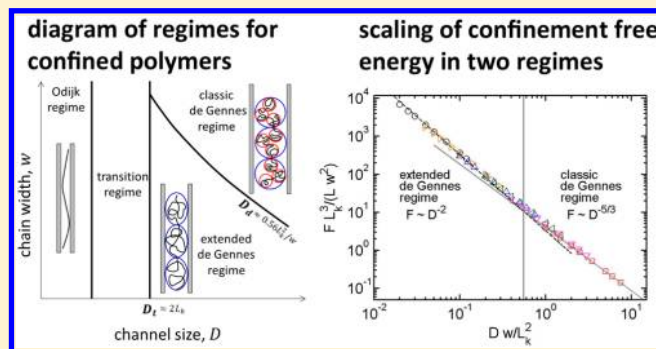
1. INTRODUCTION

The recent genomic applications of single DNA molecules in micro/nanofluidic channels has stimulated interest in polymer physics in confinement.[1−3] The behavior of polymers in the Odjik regime ($D \ll L_k$) and the de Gennes regime ($D \gg L_k$) regimes is described by the classic deflection[4] and blob[5,6] models, respectively, where D is the channel size and L_k is the Kuhn length of polymer. Unfortunately, the cross-sectional dimensions of channels in DNA experiments are typically from about L_k to several times L_k, which are located between the well-established Odjik and de Gennes regimes.[7−11] To understand DNA behavior between these two classic regimes, simulation[12−16] and theoretical studies[17−21] have been performed. However, there is no consensus among researchers regarding this important intermediate regime. Researchers have proposed the existence of an extended de Gennes regime[13,15,18] and hairpin regime.[22] Recent work[21] proposed that the extended de Gennes regime does not exist and instead suggested a universal Gauss−de Gennes regime.

Before introducing the extended de Gennes regime, we first review the blob model[5,6] for the classic de Gennes regime, where the chain is considered as a string of blobs with size of D (Figure 1). Because of excluded volume (EV) interactions, these blobs avoid each other, and the subchain within a blob follows the Flory scaling, $L_{blob} \sim D^{5/3}$, where L_{blob} is the contour length within a blob. From this description, chain extension is predicted to scale as $\langle L_\parallel \rangle \sim D^{-2/3}$, and the confinement free energy is proportional to the number of blobs $F \sim N_{blob} \sim D^{-5/3}$. To satisfy the intrablob Flory scaling and the interblob avoidance, the blob size needs to be larger than the thermal blob size L_k^2/w, where w is the effective chain width, such that the repulsion between two blobs is larger than thermal energy $k_B T$.[18] Therefore, the classic blob model is only valid for $D > D_d^* \approx L_k^2/w$.

When decreasing the channel size, we encounter a regime $L_k \ll D \ll L_k^2/w$ as initially proposed by Brochard-Wyart and Raphael.[23] This regime was named as "extended de Gennes regime" by Wang et al.[13] In this regime, an anisometric blob model was developed,[13,18,23,24] where the chain is considered as a string of *anisometric* blobs (Figure 1). The length of a blob is redefined as $R_{blob} \approx D^{2/3} L_k^{2/3} w^{-1/3}$ such that the EV interaction between two blobs equals $k_B T$, which is sufficient to segregate blobs. Using the ideal-chain scaling within anisometric blobs, the scaling of extension $L_\parallel \approx L D^{-2/3} L_k^{1/3} w^{1/3}$ [18] and the scaling of fluctuation in extension $\sigma^2 \approx L L_k$ [13] were derived and recently validated by simulations.[15]

We now consider the confinement free energy in the extended de Gennes regime, which is an important part of our
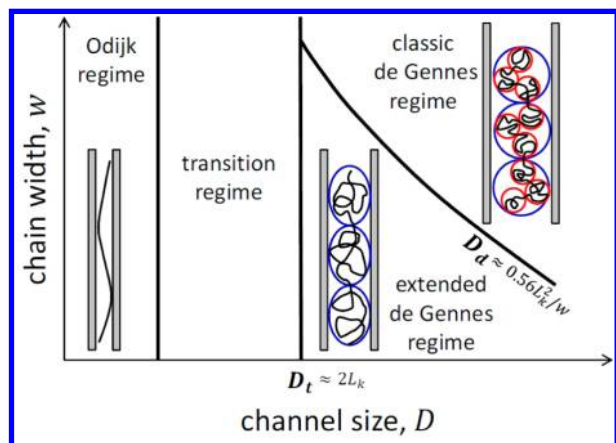
Figure 1. Schematic illustration of different regimes experienced by a long polymer in a tubular channel when varying the channel cross-sectional dimension and the chain width. D corresponds to diameter for a channel with circular cross section and width or height for a square channel. The black curves represent polymer chains, red circles represent thermal blobs, and blue circles represent the self-avoiding blobs. The boundaries between scaling regimes, D_t and D_d, are determined by our simulations presented in this work.

work. In the first study of this regime by Brochard-Wyart and Raphael,[23] the confinement free energy was proposed to be proportional to the number of anisometric blobs and then follows $F \approx LD^{-4/3}L_k^{-1/3}w^{2/3}$. Later, the same result was reached by Reisner et al.[2] using a Flory-type free energy approach. More recently, Tree et al. found that the prediction $F \approx LD^{-4/3}L_k^{-1/3}w^{2/3}$ was inconsistent with the confinement free energy calculated from simulations, which led them to reject the anisometric blob model and propose another model.[21]

In the present study, we find that the anisometric blob model itself is correct, but a wrong confinement free energy was derived from this model in previous studies.[2,21,23,25] We will first present the theoretical predictions for the extended de Gennes regime and then validate them with simulations. We demonstrate that there is indeed an extended de Gennes regime and that prior researchers were misled to cast doubt regarding its existence due to incorrectly describing the polymer free energy.[21] We will also show that this regime is analogous to what can be found in semidilute polymer solutions.

2. THEORY AND COMPUTER SIMULATION

2.1. Theory for the Extended de Gennes Regime. According to the anisometric blob model, the channel walls not only restrict the arrangement of these anisometric blobs but they also compress each anisometric blob (Figure 1). Such compression can be understood based on the fact that an anisometric blob would restore to an isotropic shape in the absence of the channel walls. The confinement free energy occurs due to restriction of interblob arrangements and compression of anisometric blobs. The first contribution is proportional to the number of blobs $N_{\text{blob}} \approx LD^{-4/3}L_k^{-1/3}w^{2/3}$. The second contribution is $N_{\text{blob}}F_{\text{com}}$, where $F_{\text{com}} \approx L_{\text{blob}}L_kD^{-2}$ is the compression energy within one blob. The term $N_{\text{blob}}F_{\text{com}}$ can be simplified to LL_kD^{-2} using $L = N_{\text{blob}}L_{\text{blob}}$, so we obtain

$$F = k_1 LD^{-4/3}L_k^{-1/3}w^{2/3} + k_2 LL_k D^{-2} \tag{1}$$

where F has been made dimensionless with k_BT, and k_1 and k_2 are order 1 dimensionless prefactors. Note that the second term corresponds to the confinement free energy of an ideal chain in

a channel. The ratio of the first term to the second term is $(Dw/L_k^2)^{2/3}$, which is vanishing small for $D \ll L_k^2/w$. The second term, as a leading term, is forgotten in previous studies.[2,21,23,25] For the first-order approximation, we have $F \approx LL_kD^{-2}$ in the extended de Gennes regime, which was also obtained before.[24] Since chain extension scales the same in the extended and classic de Gennes regimes, differences in their free energy scaling can be used to distinguish these regimes.

In addition to the blob model, the confinement free energy can be derived using another approach. In the extended de Gennes regime, we apply the traditional Flory-type free energy to calculate the confinement free energy:

$$F_{\text{Flory}} \approx \frac{LL_k}{D^2} + \frac{L_{\|}^2}{LL_k} + \frac{L^2 w}{D^2 L_{\|}} \tag{2}$$

The first term corresponds to the elastic entropy reduction due to the compression in the transversal directions. The second term corresponds to the elastic entropy reduction due to stretching in the longitudinal direction. The third term corresponds to the EV interaction. The application of above equation in the extended de Gennes regime can be justified in this way. The first two terms correspond to the free energy of an ideal chain. If we gradually increase the chain width from zero, the EV interaction would also gradually increase from zero. When the EV interaction is weak, it can be considered as a weak perturbation to the free energy of an ideal chain and can be captured by the third term in eq 2. So eq 2 should be valid in the case of weak EV interaction, i.e., the extended de Gennes regime. Minimizing the free energy with respect to the extension yields the equilibrium extension on $\langle L_{\|} \rangle \approx LD^{-2/3}L_k^{1/3}w^{1/3}$. Substituting it into eq 2, we reproduce the free energy expression $F \approx LD^{-4/3}L_k^{1/3}w^{2/3} + LL_kD^{-2}$. Recall that the compression energy within blobs LL_kD^{-2} is independent of the chain extension, and so ignoring it in previous studies[2,13] does not affect the calculation of the equilibrium extension.

We note that the confinement free energy in the extended de Gennes regime will gradually approach the case of a confined ideal chain when the chain width approaches zero. In the case of $w = 0$, eq 1 becomes $F = k_2 LL_k D^{-2}$. The confinement free energy of an ideal chain in slitlike confinement has been determined analytically with a prefactor of $(\pi^2/6)$.[26,27] For channels with square cross sections, the prefactor should be doubled, and then $k_2 = \pi^2/3$.[21] By fitting to data, we will later show that k_1 has a value of 3.0 (Figure 3c).

2.2. Computer Simulation of Polymers. To validate our predictions in the extended de Gennes regime, we apply the pruned-enriched Rosenbluth method (PERM)[28] to simulate polymers in square cross-section channels, similar to the simulations by Tree et al.[21] Two polymer models are used in our simulations: the touching-bead model and the freely jointed rod model. In the touching-bead model, the bead diameter equals the chain width. This model has been widely applied to simulate polymers under all degrees of confinement.[13,14,19–22,29] A freely jointed rod model[15] was recently developed to efficiently simulate thin chains. With this model, we can simulate much longer chains, allowing us to more fully explore the extended de Gennes regime. The diameter and the length of the rod correspond to w and L_k, respectively. These two polymer models are complementary to each other. The freely jointed rod model is suitable for simulating long and thin chains but is not applicable for strong confinement with $D \lesssim L_k$

due to the coarse-grained nature of the model. The touching-bead model is applicable for strong confinement but becomes computationally expensive to simulate long and thin chains.

We implement the PERM algorithm[28] in a manner such that we do not need an initial guess of free energy and we do not need any parameter optimization. When we use the freely jointed rod model, the chain growth starts from a rod with a random orientation. In each step of growth, a new rod with a random orientation is placed at the end of the chain. If the new rod overlaps with any other rod or the channel walls, then this chain dies. Each chain is not grown individually, but in a batch of N_c chains. The value of N_c is set to 3000, which is the maximum number allowed by our computer memory for the chain length of $L = 10^4$. Here, the chain length uses units of segments or beads. The initial weight for each chain is $1/N_c$. That is, $W_i = 1/N_c$ for $i = 1$, where i denotes the chain length. After each step of adding a rod, a few chains may die. Suppose N_d chains die. Then, we randomly pick N_d chains from $(N_c - N_d)$ survived chains and duplicate these N_d chains so that the number of chains remains at N_c during chain growth. This is the so-called enrichment. Without enrichment, the number of survived chain approaches zero, and we cannot obtain enough sampling of long chains. Considering that all survived chains have the same probability $p = N_d/(N_c - N_d)$ to be duplicated, the weights of all chains are reduced by a factor $1/(1 + p) = (N_c - N_d)/N_c$. That is, $W_{j,i+1} = W_{j,i} \times (N_c - N_d)/N_c$ after adding the $(i + 1)$-th rod to the j-th chain. When the chain length (number of rods) reaches the desired chain length $L = 10^4$, the growth stops and the final weight $W_{j,L}$ of $(N_c - N_d)$ survived chains is used to calculate the free energy of the chain in the channel $F_c = -k_B T \ \ln(\sum_{j=1}^{j=N_c-N_d} W_{j,L})$. Meanwhile, the extensions of final chains are also calculated. We run at least 100 batches such that the total number of sampled chains is at least 3×10^5 for a given chain width and channel size. The free energy and extension are averaged over these chains. Note that the weights of chains are identical in one batch but different among different batches. The standard deviations of the free energy among different batches are always around or less than $k_B T$ and typically about 0.1% of the free energy. In the touching-bead model, during chain growth the i-th bead is not added with a random orientation but added according to Boltzmann distribution of orientation energies $\exp(-E_{bend}(\theta_i)/k_B T)$, where $E_{bend}(\theta_i)/k_B T = (1/4)(L_k/w)\theta_i^2$ and θ_i is the bending angle formed by the $(i - 2)$-th, $(i - 1)$-th, and i-th beads.[14] Recall that the chain width w equals the bead diameter. The side length of the square channel D is varied from $4L_k$ to $30L_k$ when we use the freely jointed rod model or varied from $4w$ to a certain value satisfying $L_{\parallel} \approx 6D$ for the purpose of avoiding the weak confinement regime[15] when we use the touching-bead model. We also perform the chain growth simulation in bulk. The free energy in bulk F_b is subtracted from F_c to obtain the confinement free energy $F = F_c - F_b$. In addition to real chains, we perform simulations for ideal chains in square channels. In these simulations, we simply turn off the rod−rod repulsion.

To establish that these two models provide consistent results, we compare the confinement free energy obtained using two models with the same parameter set $\{w, L_k, D\}$. Figure 2 shows the confinement free energy as a function of channel size. The confinement free energy and the channel size are normalized in the same way as a previous study by Tree et al.[21] in order to directly compare results. The relative channel size is defined as $\delta \equiv D/L_p \equiv 2D/L_k$, where L_p is the persistence length equal to half of the Kuhn length L_k. Considering that the confinement
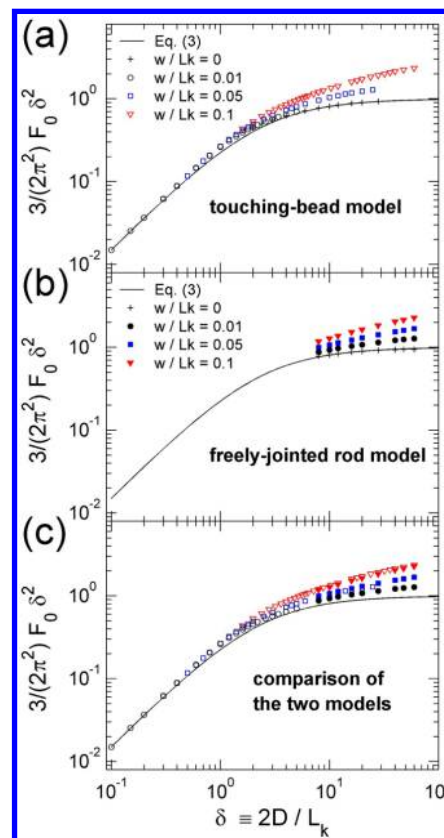

Figure 2. Normalized confinement free energy as a function of the dimensionless channel size. (a) Simulation results using the touching-bead model with 2×10^4 beads, i.e., $L/w = 2 \times 10^4$. (b) Simulation results using the freely jointed rod model with 10^4 rods, i.e., $L/L_k = 10^4$. (c) Comparison of simulation results using the two different models. The estimated statistical errors are less than symbol sizes.

free energy is proportional to the contour length, $F_0 \equiv FL_p/L \equiv FL_k/(2L)$ is defined to characterize the confinement free energy of a persistence length. The value of F_0 is normalized by $F_{ideal}^{weak} = (2/3)\pi^2\delta^{-2}$, where F_{ideal}^{weak} corresponds to the confinement free energy per L_p for an infinitely long ideal chain in weak confinement with $\delta \gg 1$.[26] In agreement with Tree et al.,[21] the plus symbols, corresponding to ideal chains, approach 1 when $\delta \gg 1$, and other symbols, corresponding to real chains, are above 1 when $\delta \gg 1$. An interpolation expression was proposed by Tree et al.[21] to approximate the confinement free energy of an ideal chain from the Odijk to de Gennes regime

$$F_{ideal} \approx \frac{(2/3)\pi^2\delta^{-2}}{(5.147\delta^{-2} + 3.343\delta^{-1} + 1)^{2/3}} \tag{3}$$

Equation 3 is also plotted in Figure 2 and agrees with our simulations of ideal chains. Figure 2c shows a comparison of the simulation results from the two models. The good agreement between the models suggests that the coarse-graining in a freely jointed rod model does not produce significant errors, at least in the overlap range of the models. It is expected that the freely jointed rod model works even better in larger channels because in the long-chain limit the freely jointed rod model gives the same end-to-end distance $(LL_k)^{1/2}$ as the wormlike chain in the absence of EV interaction.

We note the combination of the PERM method and the freely jointed rod model allows us to simulate very long and very thin chains, which are necessary to study the extended de

Gennes regime but are difficult to simulate using other methods.[13,21] Overall, our simulations allowed us prove how the transitions between various regimes and scaling of chain extension depend on w, L_k, and D.

The simulation results using the freely jointed rod model and the touching-bead model are presented in Figures 3 and 4,
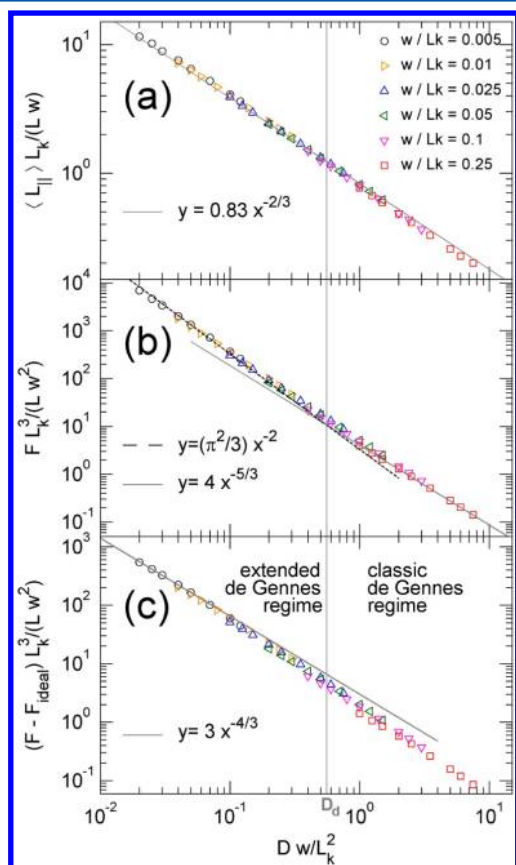

Figure 3. Results from the freely jointed rod simulations of 10^4 rods, i.e., $L/L_k = 10^4$. (a) Normalized extension as a function of normalized size of a square channel (b) Normalized confinement free energy as a function of normalized channel size. (c) The difference in confinement free energy between a real chain and an ideal chain. The crossover between the extended and classic de Gennes regimes is estimated as $D_d = 0.56L_k^2/w$. The estimated statistical errors are less than symbol sizes.

respectively. When using the freely jointed rod model, the contour length is set as $L = 10^4 L_k$, and we vary the chain width and channel sizes with respect to the Kuhn length L_k. When using the touching-bead model, the contour length is set as $L = 2 \times 10^4 w$, and we vary the Kuhn length and the channel size with respect to the chain width w. Note that the channel size D in all figures refers to the real channel size D_{real} minus the chain width w, because the quantity $D = (D_{real} - w)$ is relevant to theoretical predictions and the quantity D_{real} is relevant to experiments.

3. RESULTS AND DISCUSSION

Figure 3 shows the simulation results of $\langle L_\parallel \rangle$ and F in the extended to the classic de Gennes regime. The channel size is varied from $4L_k$ to $30L_k$. The channel size is normalized in a manner to produce universal curves that allows us to distinguish the classic and extended de Gennes regimes. In
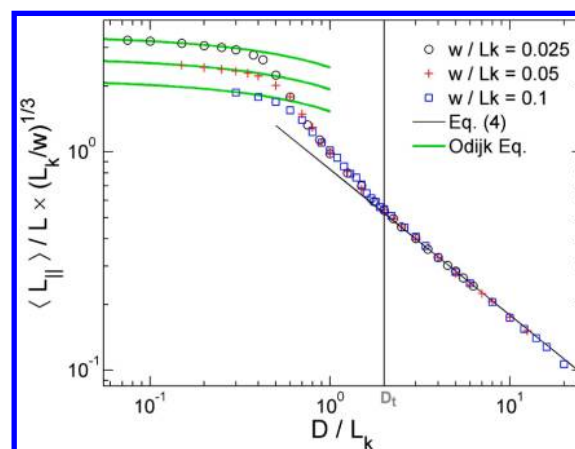

Figure 4. Normalized extension versus scaled channel size from the touching-bead model simulations. The symbols are simulation results of 2×10^4 beads using touching-bead model, i.e., $L/w = 2 \times 10^4$. The three green lines are calculated from the Odijk equation $\langle L_\parallel \rangle/L = 1 - 0.29(D/L_k)^{2/3}$.[32] The crossover between the transition regime and the extended/classic de Gennes regime is estimated as $D_t = 2L_k$. The estimated statistical errors are less than symbol sizes.

agreement with our prediction, all data points in Figure 3a follow the master equation

$$\langle L_\parallel \rangle L_k/(Lw) = 0.83(Dw/L_k^2)^{-2/3} \tag{4}$$

where the prefactor 0.83 is the best fit after setting the exponent as $-2/3$. The best power-law fit to the data points yields an exponent of -0.695 ± 0.004, which is slightly less than $-2/3$. Note that using a precise Flory scaling exponent of 0.5876[30,31] instead of 3/5 leads to the scaling $\langle L_\parallel \rangle \sim D^{-0.7018}$.

Figure 3b shows the confinement free energy. The confinement free energy is normalized to collapse the results of different chain widths. As expected, the data follow the scaling $F \sim D^{-5/3}$ for $Dw/L_k^2 > 1$. The prefactor is determined to be 4.0.

$$FL_k^3/(Lw^2) = 4.0(Dw/L_k^2)^{-5/3} \tag{5}$$

The dashed line in Figure 3b corresponds to the analytic expression for ideal chains,[26] which is expected to be always below the data points (real chains). We find that the dashed line is above a few data points because the analytic expression for ideal chains only valid for $D \gg L_k$ and overestimates F when D is only several times of L_k. The boundary between the extended and classic de Gennes regimes is then given by the intersection of the dashed and solid lines at $D_d = 0.56L_k^2/w$. The crossover from the extended to the classic de Gennes was investigated using the fluctuation in extension in our previous study, but the explicit value of D_d was not calculated previously. Extrapolating the fluctuation behaviors $\sigma^2/(LL_k) = 0.14$ and $\sigma^2/(LL_k) = 0.134(Dw/L_k^2)^{0.2982}$ in the extended and classic de Gennes regime, respectively, we obtain $D_d = 1.16L_k^2/w$. Note that in our previous study of fluctuation behaviors the channel cross sections are circles and D corresponds to the diameter. In the current study, the cross sections of channels are square and D corresponds to the side length of the square.

To examine in more detail the extended de Gennes regime, we plot the difference between the confinement free energy of a real chain and an ideal chain in Figure 3c because in the extended de Gennes regime eq 1 can be converted to

$$(F - F_{ideal})L_k^3/(Lw^2) \approx (Dw/L_k^2)^{-4/3} \qquad (6)$$

F_{ideal} was calculated from simulations rather than the analytic expression since channel dimension go down to $D = 4L_k$. As expected, the scaling exponent approaches $-4/3$ when $Dw/L_k^2 \ll 1$. The value of $(F - F_{ideal})$ in Figure 3c is 1 order of magnitude less than the value of F in Figure 3b, which is consistent with our prediction that F_{ideal} dominates the confinement free energy in the extended de Gennes regime.

It is intriguing that in the extended de Gennes regime the chain exhibits real-chain behavior globally (interblob) but exhibits ideal-chain behavior locally (intrablob). In this regime, the chain extension, depending on the interblob organization, follows the real-chain scaling. On the other hand, the confinement free energy, mainly depending on the intrablob organization, follows the ideal-chain scaling $F \approx LL_kD^{-2}$.

The upper bound of channel size D_d for the extended de Gennes regime is determined by Figure 3. To determine the lower bound of channel size D_t, we perform simulations from the classic/extended de Gennes regime to the Odijk regime using touching-bead model. Figure 4 shows the extension as a function of the relative channel size, while the extension is normalized to collapse data points of different chain widths in the classic/extended de Gennes regime. The data for $D > 2L_k$ follow the scaling $\langle L_\parallel \rangle \sim D^{-2/3}$ and agree with eq 4, which is determined from simulations using the freely jointed rod model. The agreement suggests the coarse-graining in the freely jointed rod model induces little error. The critical channel size D_t, where $\langle L_\parallel \rangle$ starts to deviate from eq 4, is around $2L_k$, which is insensitive to the chain width. Note that Tree et al. predicted $D_t \sim w^{-1}$, which is inconsistent with our observation. It is worth mentioning that our simulation results agree with the results by Tree et al., but Tree et al. failed to determine the correct D_{min} because they did not make a plot with the same normalization as Figure 3. When $L_k < D < 2L_k$, the apparent exponent is about -1, in agreement with many other simulations[12,13,33] and experiments.[8,11,34] In strong confinement, the extension follows the Odijk equation $\langle L_\parallel \rangle/L = 1 - 0.29(D/L_k)^{2/3}$.[32]

We note that the extended de Gennes regime for confined semiflexible chains is similar to the semidilute marginal condition proposed and studied by Schaefer et al.[36] and Birshtein,[36] which is shown in Figure 5. Applying the classic blob model, a chain in the semidilute solution is viewed as a string of blobs.[37] Intrablob conformations follow real-chain behavior, while interblob conformations follow ideal-chain

Figure 5. Diagram of regimes for polymer solutions. Adapted from Figure 3 in the paper by Shaefer et al.[35]

behavior because the space is fully filled by the blobs. As in the extended de Gennes regime, the intrablob conformations should deviate from real-chain behavior when EV interactions inside a blob is weaker than k_BT. Such situation was investigated and termed as semidilute marginal condition by Schaefer et al.[35] They determined the critical concentration $\tilde{\rho} \approx w/L_k^4$ of Kuhn segments, and furthermore, they found a new characteristic length $\xi \approx w^{-1/2}c^{-1/2}$ in monomer–monomer pair-correlation $g(r) \sim (1/r)\exp(-r/\xi)$. We found that $\tilde{\rho}$ and ξ for the semidilute marginal condition perfectly match the critical channel size D_d and the length of anisometric blob R_{blob} for the extended de Gennes regime. It is easy to derive that when $D_d = L_k^2/w$, the concentration of Kuhn segments in the channel is $c = (L/L_k)/(L_\parallel D^2) \approx w/L_k^4$, which shares the same expression with $\tilde{\rho}$. Furthermore, using $c = (L/L_k)/(L_\parallel D^2)$ and $L_\parallel \approx LD^{-2/3}L_k^{1/3}w^{1/3}$, we obtain the relationship $D \approx c^{-3/4}L_k^{-1}w^{-1/4}$. Substituting it into $R_{blob} \approx D^{2/3}L_k^{2/3}w^{-1/3}$, we arrive at $R_{blob} \approx w^{-1/2}c^{-1/2}$, which shares the same expression with ξ. Compared to the semidilute marginal condition,[38,39] the extended de Gennes regime is easier to be validated and identified by simulations and experiments, such as measuring the fluctuation in extension of confined DNA.

Broadly speaking, the separation of the extended/classic de Gennes regimes is caused by the competition of EV interaction to thermal energy. Such competition also leads to the separation of the extended/classic Pincus regimes for a polymer under tension.[15,40] If we compress or stretch a polymer in a channel, the polymer may experience a transition between a weak-EV regime to a strong-EV regime, and the scaling behavior is expected to change, such as the relaxation time.[13,15]

A key application of the correct confinement free energy in the extended de Gennes regime is to calculate the recoiling force f_{recoil}, which needs to be overcome when driving a chain into a channel.[41,42] Applying the expressions of F and $L_\parallel$ in the extended de Gennes regime, we derive $f_{recoil} = F/L_\parallel = (D^{-2/3}L_k^{-2/3}w^{1/3} + D^{-4/3}L_k^{2/3}w^{-1/3})k_BT \approx D^{-4/3}L_k^{2/3}w^{-1/3}k_BT$, which is different from the expression from the wrong confinement free energy.[25]

4. CONCLUSIONS

In summary, we for the first time derive the correct confinement free energy in the extended de Gennes regime using the anisometric blob model and validate it by simulations using a newly developed polymer model. Theoretically, the extended de Gennes regime is a specific case of a common polymer system where EV interactions are weak and behavior of the chain is neither purely real nor ideal Practically, our results provide theoretical basis for the practical applications of microfluidic/nanofluidic devices to stretch DNA,[7,43−46] such as the relationship between the chain extension and channel size, and the calculation of required force to drive DNA into channels.

■ AUTHOR INFORMATION

Corresponding Author
*E-mail: pdoyle@mit.edu (P.S.D.).

Notes
The authors declare no competing financial interest.

■ REFERENCES

(1) Dorfman, K. D. *Rev. Mod. Phys.* **2010**, *82*, 2903−2947.
(2) Reisner, W.; Pedersen, J. N.; Austin, R. H. *Rep. Prog. Phys.* **2012**, *75*, 106601.
(3) Dorfman, K. D.; King, S. B.; Olson, D. W.; Thomas, J. D. P.; Tree, D. R. *Chem. Rev.* **2013**, *113*, 2584−2667.
(4) Odijk, T. *Macromolecules* **1983**, *16*, 1340−1344.
(5) Daoud, M.; de Gennes, P. G. *J. Phys. (Paris)* **1977**, *38*, 85.
(6) de Gennes, P. G. *Scaling Concepts in Polymer Physics*; Cornell University Press: Ithaca, NY, 1979.
(7) Tegenfeldt, J. O.; Prinz, C.; Cao, H.; Chou, S.; Reisner, W. W.; Riehn, R.; Wang, Y. M.; Cox, E. C.; Sturm, J. C.; Silberzan, P.; Austin, R. H. *Proc. Natl. Acad. Sci. U. S. A.* **2004**, *101*, 10979−10983.
(8) Reisner, W.; Morton, K. J.; Riehn, R.; Wang, Y. M.; Yu, Z.; Rosen, M.; Sturm, J. C.; Chou, S. Y.; Frey, E.; Austin, R. H. *Phys. Rev. Lett.* **2005**, *94*, 196101.
(9) Balducci, A.; Mao, P.; Han, J. Y.; Doyle, P. S. *Macromolecules* **2006**, *39*, 6273−6281.
(10) Bonthuis, D. J.; Meyer, C.; Stein, D.; Dekker, C. *Phys. Rev. Lett.* **2008**, *101*, 108303.
(11) Persson, F.; Utko, P.; Reisner, W.; Larsen, N. B.; Kristensen, A. *Nano Lett.* **2009**, *9*, 1382−1385.
(12) Cifra, P. *J. Chem. Phys.* **2009**, *131*, 224903.
(13) Wang, Y.; Tree, D. R.; Dorfman, K. D. *Macromolecules* **2011**, *44*, 6594−6604.
(14) Dai, L.; Jones, J. J.; van der Maarel, J. R. C.; Doyle, P. S. *Soft Matter* **2012**, *8*, 2972−2982.
(15) Dai, L.; Doyle, P. S. *Macromolecules* **2013**, *46*, 6336.
(16) Werner, E.; Persson, F.; Westerlund, F.; Tegenfeldt, J. O.; Mehlig, B. *Phys. Rev. E* **2012**, *86*, 041802.
(17) Odijk, T. *J. Chem. Phys.* **2006**, *125*, 204904.
(18) Odijk, T. *Phys. Rev. E* **2008**, *77*, 060901.
(19) Tree, D. R.; Wang, Y.; Dorfman, K. D. *Phys. Rev. Lett.* **2012**, *108*, 228105.
(20) Dai, L.; Tree, D. R.; van der Maarel, J. R.; Dorfman, K. D.; Doyle, P. S. *Phys. Rev. Lett.* **2013**, *110*, 168105.
(21) Tree, D. R.; Wang, Y.; Dorfman, K. D. *Phys. Rev. Lett.* **2013**, *110*, 208103.
(22) Dai, L.; Ng, S. Y.; Doyle, P. S.; van der Maarel, J. R. C. *ACS Macro Lett.* **2012**, *1*, 1046−1050.
(23) Brochard-Wyart, F.; Raphael, E. *Macromolecules* **1990**, *23*, 2276.
(24) Brochard-Wyart, F.; Tanaka, T.; Borghi, N.; de Gennes, P.-G. *Langmuir* **2005**, *21*, 4144.
(25) Taloni, A.; Yeh, J. W.; Chou, C. F. *Macromolecules* **2013**, *46*, 7989.
(26) Casassa, E. F. *J. Polym. Sci., Part B: Polym. Lett.* **1967**, *5*, 773.
(27) Chen, J. Z. Y.; Sullivan, D. E. *Macromolecules* **2006**, *39*, 7769−7773.
(28) Grassberger, P. *Phys. Rev. E* **1997**, *56*.
(29) Dai, L.; van der Maarel, J. R. C.; Doyle, P. S. *ACS Macro Lett.* **2012**, *1*, 732−736.
(30) Li, B.; Madras, N.; Sokal, A. D. *J. Stat. Phys.* **1995**, *80*, 661−754.
(31) Clisby, N. *Phys. Rev. Lett.* **2010**, *104*, 055702.
(32) Yang, Y. Z.; Burkhardt, T. W.; Gompper, G. *Phys. Rev. E* **2007**, *76*, 011804.
(33) Cifra, P.; Benkova, Z.; Bleha, T. *J. Phys. Chem. B* **2009**, *113*, 1843−1851.
(34) Utko, P.; Persson, F.; Kristensen, A.; Larsen, N. B. *Lab Chip* **2011**, *11*, 303−308.
(35) Schaefer, D. W.; Joanny, J. F.; Pincus, P. *Macromolecules* **1980**, *13*, 1280.
(36) Birshtein, T. M. *Polym. Sci. U. S. S. R.* **1982**, *24*, 2416.

(37) Daoud, M.; Cotton, J. P.; Farnoux, B.; Jannink, G.; Sarma, G.; Benoit, H.; Duplessix, C.; Picot, C.; de Gennes, P. G. *Macromolecules* **1975**, *8*, 804.
(38) Shafran, E.; Yaniv, A.; Krichevsky, O. *Phys. Rev. Lett.* **2010**, *104*, 128101.
(39) Nepal, M.; Yaniv, A.; Shafran, E.; Krichevsky, O. *Phys. Rev. Lett.* **2013**, *110*, 058102.
(40) McIntosh, D. B.; Ribeck, N.; Saleh, O. A. *Phys. Rev. E* **2009**, *80*.
(41) Reisner, W.; Larsen, N. B.; Flyvbjerg, H.; Tegenfeldt, J. O.; Kristensen, A. *Proc. Natl. Acad. Sci. U. S. A.* **2009**, *106*, 79−84.
(42) Yeh, J. W.; Taloni, A.; Chen, Y. L.; Chou, C. F. *Nano Lett.* **2012**, *12*, 1597−1602.
(43) Reisner, W.; Larsen, N. B.; Silahtaroglu, A.; Kristensen, A.; Tommerup, N.; Tegenfeldt, J. O.; Flyvbjerg, H. *Proc. Natl. Acad. Sci. U. S. A.* **2010**, *107*, 13294−13299.
(44) Jo, K.; Dhingra, D. M.; Odijk, T.; de Pablo, J. J.; Graham, M. D.; Runnheim, R.; Forrest, D.; Schwartz, D. C. *Proc. Natl. Acad. Sci. U. S. A.* **2007**, *104*, 2673−2678.
(45) Lam, E. T.; Hastie, A.; Lin, C.; Ehrlich, D.; Das, S. K.; Austin, M. D.; Deshpande, P.; Cao, H.; Nagarajan, N.; Xiao, M.; Kwok, P. Y. *Nat. Biotechnol.* **2012**, *30*, 771−776.
(46) Marie, R.; Pedersen, J. N.; Bauer, D. L.; Rasmussen, K. H.; Yusuf, M.; Volpi, E.; Flyvbjerg, H.; Kristensen, A.; Mir, K. U. *Proc. Natl. Acad. Sci. U. S. A.* **2013**, DOI: 10.1073/pnas.1214570110.